Transactions of the Materials Research Society of Japan 29 [8] 3719-3722 (2004)

Electronic Structures of the TTTA Molecular Crystal

Miou Furuya[1], Kaoru Ohno[1], Jun Takeda[1] and Yoshiyuki Kawazoe[2]
[1]Department of Physics, Graduate School of Engineering, Yokohama National University,
79-5 Tokiwadai, Hodogaya-ku, Yokohama 240-8501, Japan
Fax: 81-45-338-3020, e-mail: d02gd227@ynu.ac.jp, ohno@ynu.ac.jp, jun@ynu.ac.jp
[2]Institute for Materials Research, Tohoku University, 2-1-1 Katahira, Aoba-ku, Sendai 980-8577
Fax: 81-22-215-2052, e-mail: kawazoe@imr.edu

Recently Fujita and Awaga found that the crystal made of organic radical, 1,3,5-trithia-2,4,6-triazapentalenyl (TTTA), exhibits a large first-order magnetic and structural phase transition between a paramagnetic high-temperature (HT) phase and a diamagnetic low-temperature (LT) phase, with a surprisingly wide thermal hysteresis loop over the temperature range 230-305K. We investigated theoretically the crystal structures for the two phases by means of the ab-initio molecular dynamics method based on the local density approximation. The resulting structures are in excellent agreement with the recent X-ray diffraction experiment. In the HT phase, uniform one-dimensional stacking of the radical molecules appears, while, in the LT phase, strong dimerization along the stacking direction appears. Because of this dimerization, core levels are doubled by splitting. From the same reason, 0.8eV band gap exists in the LT phase, while Fermi level exists in the HT phase. This is the origin of the diamagnetism and paramagnetism, respectively, in the LT and HT phases. We also estimated Raman and IR frequencies of this molecule theoretically.
Key words: molecular crystal, *ab initio* method, band structure, dielectric response function, and reflection spectrum

1. INTRODUCTION

Recently molecule-based materials have been studied with much interest because of their potential in the future application to nano-scale electronic, magnetic and optical devices. An organic radical, TTTA (1,3,5-trithia-2,4,6- triazapentalenyl), offers a good example of the crystal composed of an organic radical molecule. As shown in Fig. 1, TTTA has a flat heterocyclic triazyl structure. Fujita and Awaga [1] found that the TTTA crystal exhibits a first-order phase transition between a paramagnetic high-temperature (HT) phase and a diamagnetic low-temperature (LT) phase, with a surprisingly wide thermal hysterisis loop near the room temperature. They also determined the crystal structures of both phases by the X-ray diffraction experiment [1,2]. Recently Takeda *et al.* found also experimentally that a photo-induced magnetic phase transition takes place in this system and its magnetic properties can be optically controlled [3] .

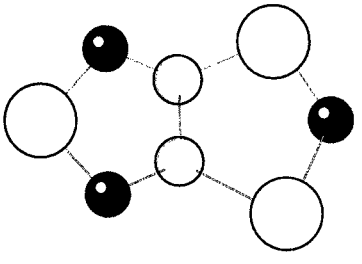

Fig. 1 Structure of TTTA molecule. Large white spheres represent sulfurs atoms, and small white and dark spheres represent carbon and nitrogen atoms, respectively.

In the present paper, we carry out the structural optimization and the electronic structure calculations for both phases of the TTTA crystal and determine the band diagrams including core levels. In the LT phase, we discuss the existence of the band gap and calculate the reflection spectrum. For all these calculations, we adopt the *ab initio* methods within the local density approximation (LDA) in density functional theory. We also calculated Raman spectrum of a TTTA molecule and compared it with the recent experiment [3].

2. RESULTS

We have carried out the structural optimization for the both phases of the TTTA crystal in the following way. Assuming the crystal symmetries (the HT phase belongs to the monoclinic $P2_1/c$ and the LT phase belongs to the triclinic $P\bar{1}$), lattice constants and angles of the unit cell given by the X-ray diffraction measurement [1], we optimized all atomic positions inside the unit cell by means of the standard *ab initio* ultrasoft-pseudopotential approach (VASP) [4] with the 26 Ry cutoff energy for the plane waves (PW's). From this calculation, we have confirmed that the position data determined experimentally [2] are reproduced within the error of 0.09 Å. The resulting structures are shown in Figs. 2a and 2b, respectively, for the HT and LT phases. The estimated total energy difference between the two phases is 0.31 eV.

Here we briefly summarize the characteristics of the crystal structures for the HT and LT phases. There is a crucial difference in molecular packing in the two phases: The molecular planes are all parallel in the HT phase (Fig. 2a), whereas the unit cell of the LT phase

includes two molecular-plane orientations (Fig. 2b). In addition, in the HT phase, uniform one-dimensional stacking of the radical molecules appears, while, in the LT phase, strong dimerization along the stacking direction appears.

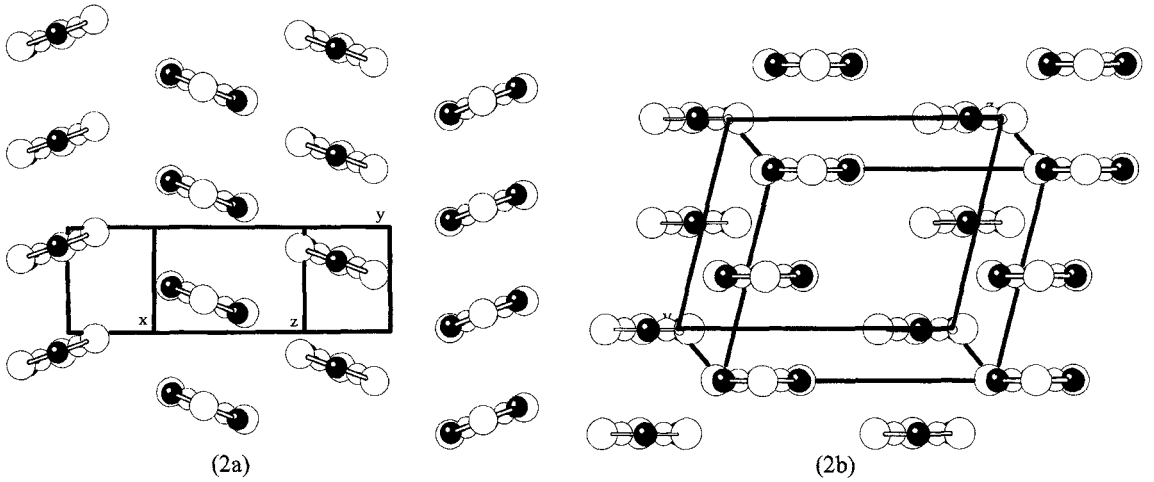

(2a) (2b)

Fig. 2 Side views of (a) the columnar structure in the HT phase whose crystal structure is monoclinic, and (b) the dimerized structure in the LT phase whose crystal structure is triclinic.

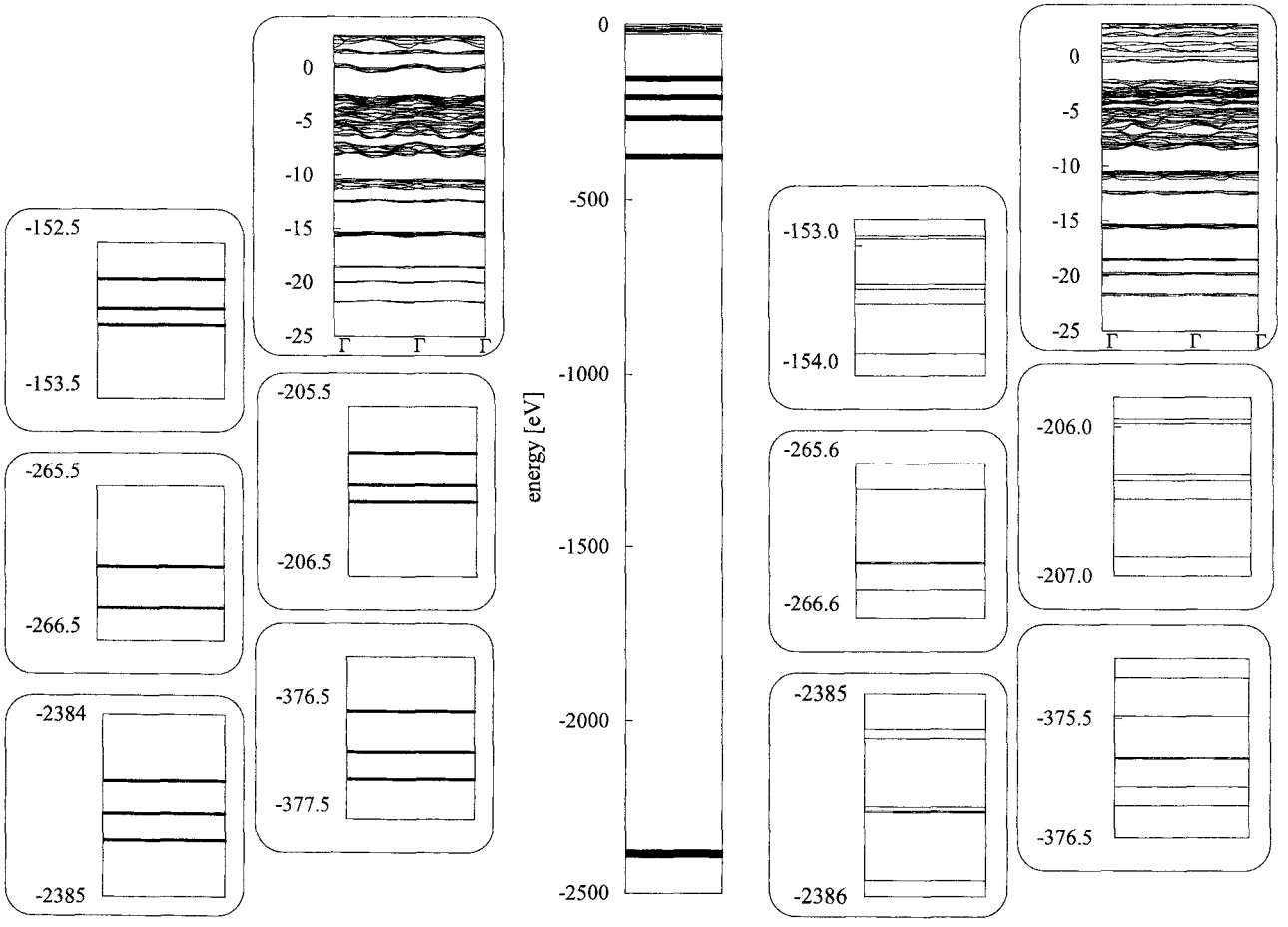

(3a) (3b)

Fig. 3 Band structures of (a) the HT phase and (b) the LT phase. They show calculated valence and deep core levels, which indicate, from top to bottom, valence levels, sulfur 2p, sulfur 2s, carbon 1s, nitrogen 1s and sulfur 1s levels, respectively. One can find out band doubly splitting from the HT phase to LT phase.

For the following electronic structure calculations, we used the all-electron mixed basis approach [5-7] using both PW's and atomic orbitals (AO's) as a basis set. Here all the core and valence AO's are determined numerically within the non-overlapping atomic spheres by a standard atomic program in Herman-Skillman's framework with the logarithmic radial mesh. For the LDA exchange- correlation functional, we adopt the Ceperley-Alder fitting form [8]. For the present system, we use 208 numerical AO's and 2135 (in the HT phase) or 2401 (in the LT phase) PW's corresponding to a 12 Ry cutoff energy using 36 special k points.

The resulting band structures are shown in Figs. 3a and 3b, respectively, for the HT and LT phases. Fermi level exists in the HT phase (Fig. 3a). In the LT phase (Fig. 3b), because of the dimerization of TTTA molecules, all two-fold degenerated levels including core levels split into two separate levels and 0.8eV band gap appears. This clear distinction of the band diagrams must be the origin of Pauli's spin paramagnetism (for a metal) in the HT phase and the closed-shell diamagnetism (for an insulator) in the LT phase.

From Figs. 2a and 2b, we know that the structural phase transition between the HT and LT phases is due to the Jahn-Teller effect, because the static Jahn-Teller effect occurs when the highest occupied level is degenerate and occupied partially by electrons. The crystal is distorted spontaneously in order to gain the energy by removing the degeneracy. In the present case, this lattice distortion is characterized by the dimerization of molecules and the corresponding phase transition can be regarded as a kind of Peierls transition.

In the present LDA picture, the Fermi level exists in the HT phase. The HT phase is, however, not optically a metal in experiments. We can argue that the strong electron-electron Coulomb repulsion and the existence of the partially filled bands near the Fermi level induce a Mott-Hubbard insulator, i.e., a paramagnetic insulator. We estimated the on-site Coulomb energy of the HT phase to be about 6.7 eV, whereas bandwidth is not more than 1eV. We found by carrying out a calculation based on the local spin density approximation (LSDA) instead of the LDA that the four levels around Fermi level break up into two full-filling majority spin levels and two empty minority spin levels, resulting in the spin polarization. This suggests that the instability of the present LDA ground state may occur by the perturbation due to the electron correlation.

In the LT phase, the frequency and wave-number dependent dielectric response function is calculated within the random phase approximation (RPA) [9]. Figure 4 represents the resulting reflection spectra in the LT phase. The thin and thick curves represent the reflection spectra for the electric field $\boldsymbol{E}$ of lights parallel and perpendicular to the stacking axis, respectively. If we compare Fig. 4 with the experimental reflection spectra [2], we find close similarity in the overall behavior, although there is difference in peak positions and amplitudes: The large peak at 1.5 eV in the thick curve ($\boldsymbol{E}$ // stacking direction) corresponds the experimental peak at 2.2 eV, while the two peaks at 1.8 eV and at 3.2 eV in the thin curve ($\boldsymbol{E}$ $\perp$ stacking direction) corresponds to the experimental peaks at 1.9 eV and at 3.4 eV.

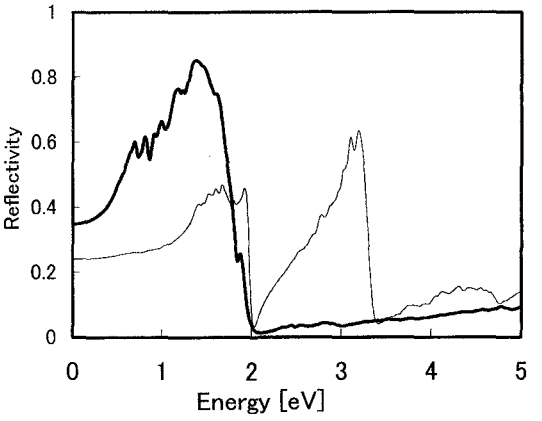

Fig. 4 Reflectivity spectrum in the LT phase. The thin and thick curves represent the results with the electric field **E** of the lights parallel (thick curve) and perpendicular (thin curve) to the stacking axis, respectively.

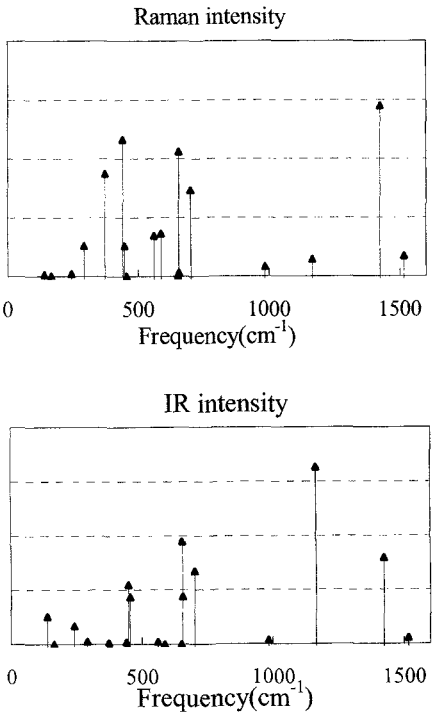

Fig. 5 Calculated Raman and IR spectrum of a TTTA molecule.

In order to confirm that the photo induced magnetic phase transition really occurs on TTTA, Takeda et al. [3] measured Raman spectra of the HT and LT phases. The Raman spectrum of the HT phase consists of mainly four vibrational modes (434.3, 501.8, 681.1 and 779.5 cm^{-1}), while that of the LT phase shows a lot of vibrational modes. Here we calculated the Raman and IR frequencies of TTTA molecule by using a GAUSSIAN 98 package program with the exchange correlation of B3-LYP and the basis functions of atoms, 6-311 †g. Since TTTA molecule consists of eight atoms, 18 vibrational modes are found as shown in Fig. 5. Although the observed Raman frequencies of the HT phase are not in good

agreement with the calculated ones, there is an overall correspondence with respect to peak positions and heights. The observed strong vibrational modes around 1350 cm^{-1} and those around 400-800 cm^{-1} may be attributed to the C=N stretching and S-N stretching modes in a planar molecular structure of TTTA, respectively.

3. SUMMARY

We have investigated structural and electronic properties of TTTA molecule and its crystalline phases, by means of the first-principles calculations. We have explicitly given the band structure diagrams including core levels which may be compared with UPS and XPS experiments. We have calculated the reflectivity spectrum in the LT phase and the Raman and IR spectra of TTTA molecule. The results were compared with available experimental data and good correspondence was obtained.

ACKNOWLEDGEMENTS

The authors would like to thank Prof. Awaga for helpful discussions. The authors acknowledge the support of the HITAC SR8000 supercomputing facilities that are owned by the Computer Science Group at the Institute for Materials Research, Tohoku University. This work was supported in part by a Grand-in-Aid for Scientific Research B (No. 15340094) from Japan Society for the Promotion of Science (JSPS).

REFERENCES

[1] W. Fujita and K. Awaga: SCIENCE Vol. **286,** 261 (8 October 1999) .
[2] W. Fujita, K. Awaga, H. Matsuzaki and H. Okamoto, Phys. Rev. B 65, 064434 (2002).
[3] J. Takeda, M. Imae, O. Hanado, S. Kurita, M. Furuya, K. Ohno, and T. Kodaira: Chem. Phys. Lett. 378 (2003) 456-462.
[4] G. Kresse and J. Furthmüller, Comput. Mater. Sci. **6**, 15 (1996); Phys. Rev. B **54**, 11 169 (1996).
[5] K. Ohno, Y. Maruyama, K. Esfarjani, Y, Kawazoe, N. Sato, R. Hatakeyama, T. Hirata, and M. Niwano, Phys. Rev. Lett. **76**, 3590 (1996).
[6] K. Ohno, F. Marui and S. G. Louie, Phys. Rev. B **56**, 1009 (1997).
[7] S. Ishii, K. Ohno and Y. Kawazoe, Mater. Trans. JIM **40**, 1209 (1999).
[8] D. M. Ceperley and B. J. Alder, Phys. Rev. Lett. **45**, 566 (1980).
[9] M. Furuya, K. Ohno, T. Morisato, Y. Kawazoe, and J. Takeda, Trans. MRSJ 28, [3], 911 (2003).

(Received October 13, 2003; Accepted April 24, 2004)